Journal of The Electrochemical Society, **155** (1) D35-D39 (2008)
0013-4651/2007/155(1)/D35/5/$23.00 © The Electrochemical Society

HF Species and Dissolved Oxygen on the Epitaxial Lift-Off Process of GaAs Using AlAsP Release Layers

A. T. J. van Niftrik,[a,z] J. J. Schermer,[a] G. J. Bauhuis,[a] P. Mulder,[a] P. K. Larsen,[a] M. J. van Setten,[b] J. J. Attema,[b] N. C. G. Tan,[c] and J. J. Kelly[d,*]

[a]*Applied Materials Science, Institute for Molecules and Materials,* [b]*Electronic Structure of Materials, Institute for Molecules and Materials, and* [c]*Department of Microbiology, Institute for Wetland and Water Research, Radboud University Nijmegen, 6525 ED Nijmegen, The Netherlands*
[d]*Condensed Matter and Interfaces, Debye Institute, Utrecht University, 3508 TA Utrecht, The Netherlands*

The lateral etch rate of the epitaxial lift-off (ELO) process was determined as a function of the total HF concentration C_{HF} and the O_2 partial pressure P_{O_2}. For this purpose samples were grown by metallorganic chemical vapor deposition and etched using a weight-induced ELO process. It was found that the etch rate increases linearly with C_{HF}, which is in accordance with the model on the ELO process presented in a previous paper. This result and composition calculations of HF solutions show that the first step in the etch process of AlAs with an HF solution most probably takes place by chemical attack of undissociated HF on AlAs surface bonds. Furthermore, it is shown that the ELO rate increases slightly over a P_{O_2} range varying from 0.046 to 0.98 atm and that for $P_{O_2} = 0.003$ atm, a significantly lower etch rate is found. We suggest that the observed decrease is the result of surface passivation by elemental arsenic, which is formed by the reaction of AlAs with H^+. An oxygen-poor atmosphere may allow the build-up of elemental arsenic on the surface, thus slowing down the AlAs reaction with HF. Oxygen, by removing arsenic as As_2O_3, keeps the surface active.
© 2007 The Electrochemical Society. [DOI: 10.1149/1.2799737] All rights reserved.

Manuscript submitted May 31, 2007; revised manuscript received September 10, 2007.
Available electronically November 6, 2007.

The epitaxial lift-off (ELO) technique, in which a III/V device structure is separated from its GaAs substrate by using selective wet etching of a thin $Al_xGa_{1-x}As$ ($x > 0.6$) release layer and transferred to a foreign carrier, allows the production of single-crystalline thin films of III/V materials.[1] Application of this technique is interesting for the optoelectronics industry because use of thin-film devices results potentially in a more efficient transfer of generated heat from device to carrier or heat sink and significantly reduces the amount of material needed by reuse of the substrates.[2] This is of particular importance for intrinsically large-areas, thus expensive, devices like high-efficiency III/V solar cells,[2,3] and the integration of III/V-based components with, for example, silicon-based devices.[4,5] Recently, at our institute thin-film GaAs solar cells, based on the ELO technique, reached record efficiencies of 24.5%.[6] This is close to the highest efficiency of 25.1% reported for regular GaAs cells on a GaAs substrate,[7] which indicates that this technique is not detrimental to the quality of the thin-film device.

In the ELO process (see Fig. 1a) the AlAs release layer is etched with hydrofluoric acid (HF), which leads to the formation of gaseous arsine (AsH_3), solid aluminum fluoride ($AlF_3 \cdot 3H_2O$), and dissolved aluminum fluoride complexes as the major reaction products.[8] This reaction is most likely described by a set of overall reactions given by

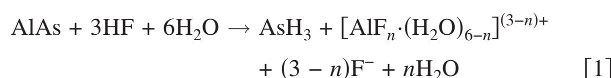

$$\mathrm{AlAs + 3HF + 6H_2O \rightarrow AsH_3 + [AlF_n \cdot (H_2O)_{6-n}]^{(3-n)+} + (3-n)F^- + nH_2O} \quad [1]$$

with $n = 0,1,2,3$. In a previous work,[9] the ELO process was described by a diffusion and reaction related model (DR-model), which is based on the notion that the overall etch rate V_e is determined by both the diffusion of HF to the etch front and its subsequent reaction (see Fig. 1b). According to this model V_e is given by

$$V_e = \frac{[\mathrm{HF}]_{l=L}}{R_d + R_r} \quad [2]$$

in which $[\mathrm{HF}]_{l=L}$ is the HF concentration in the bulk of the solution and $R_d + R_r$ the resistance of the etch process. The total resistance consists of a diffusion and a reaction related resistance, respectively R_d and R_r, which can be expressed as

$$R_d = \frac{\pi\sqrt{rh}3[\mathrm{AlAs}]}{\sqrt{2}D_0} \exp\left(\frac{E_{a,d}}{k_B T}\right) \quad [3]$$

and

$$R_r = \frac{1}{A} \exp\left(\frac{E_{a,r}}{k_B T}\right) \quad [4]$$

where r is the radius of curvature of the thin film, h the release layer thickness, $[\mathrm{AlAs}]$ the molar concentration of solid AlAs, D_0 the

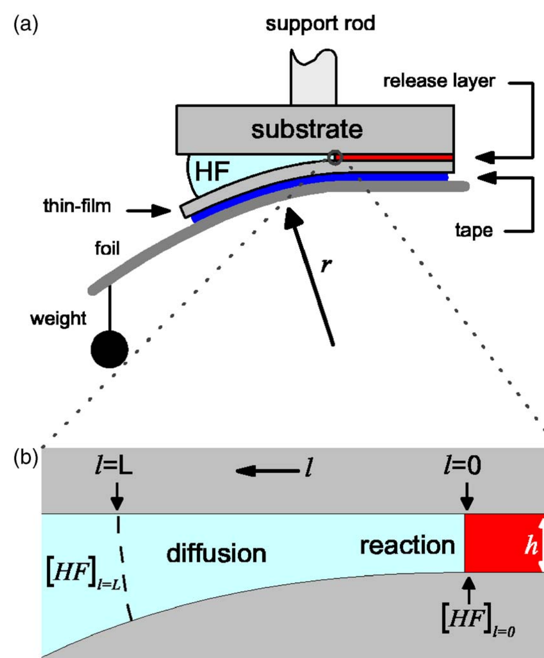

Figure 1. (Color online) Schematic cross section of the (a) weight-induced ELO setup, and (b) detail of (a) indicating the diffusion and reaction regime of the process. The concentration of HF is lowest at the etch front, where it is consumed ($[\mathrm{HF}]_{l=0}$) and gradually increases with the distance from the etch front until the bulk concentration ($[\mathrm{HF}]_{l=L}$) is reached at a certain distance $l = L$. Note that the dimensions are not to scale.

* Electrochemical Society Active Member.
[z] Email: Ton.vanNiftrik@science.ru.nl

Downloaded 16 Jan 2009 to 131.211.45.133. Redistribution subject to ECS license or copyright; see http://www.ecsdl.org/terms_use.jsp

diffusion coefficient at infinite temperature, $E_{a,d}$ the activation energy associated with the diffusion of HF, k_B the Boltzmann constant, T the temperature, A the Arrhenius constant and $E_{a,r}$ the activation energy of the surface reaction. The DR-model was tested by several series of experiments, which showed that the ELO etch rate is reaction rate related by its dependence on the composition of the release layer, and diffusion rate related by its dependence on the thickness of the release layer. In contrast to the model that was previously described in the literature,[4,10] it was found that the DR-model yields etch rates that are in quantitative agreement with those obtained experimentally.

In 2002, bulk etch experiments[11] showed that the etch rate of $Al_xGa_{1-x}As$ ($0.65 \leq x \leq 1.0$) layers depends linearly on the HF concentration, which is in accordance with the DR-model (see Eq. 2). It should be noted, however, that this result was obtained over a relatively small range of HF volume percentages (1–10%). Aqueous HF solutions with a HF percentage up to 48% are commercially available. This corresponds to a total HF concentration C_{HF} of 24 mol kg^{-1}. In an aqueous solution, HF can give rise to H^+, F^-, HF_2^-, and $H_2F_3^-$ and the composition of the HF solution may vary strongly with C_{HF}. Therefore, in the present work the ELO process was studied over a wide range of C_{HF}–values.

Another bulk etch study[8] showed that oxygen (O_2) is required to maintain the AlAs etch process with HF. Therefore, in the present work a second series of experiments was performed to study the ELO etch rate as a function of the O_2 concentration.

Experimental

All samples examined in this study were grown on 2 in. diam undoped GaAs wafers with crystal orientation (001), 2° off toward ⟨110⟩ using low-pressure metallorganic chemical vapor deposition (MOCVD) in a horizontal Aixtron 200 reactor. Source materials were trimethyl-gallium and trimethyl-aluminum as group-III precursors and arsine and phosphine as group-V precursors. Disilane was used as dopant precursor to obtain n-type doping for the release layer; all other layers were undoped. Each growth run was performed at a temperature of 650°C and a pressure of 20 mbar.

In the past, the ELO process was generally performed with $Al_xGa_{1-x}As$ ($x > 0.6$) release layers. In previous work,[9] however, it was shown that a similar etch behavior was found for $AlAs_{1-y}P_y$ ($0 \leq y \leq 0.8$) release layers. Furthermore, it was found that the ELO etch rate is highest for $AlAs_{1-y}P_y$ release layers with a P content of 2–3% and a release layer thickness of 10 nm. Therefore, layer structures were grown with a 10 nm thick $AlAs_{0.98}P_{0.02}$ release layer between the GaAs top layer and GaAs substrate (plus buffer layer), as shown in Fig. 2. The $AlAs_{0.98}P_{0.02}$ release layer was deposited at a rate of ~1.5 μm h^{-1} (V/III ratio = 204), and the GaAs layers were grown at 1.87 μm h^{-1} (V/III ratio = 121). The solid composition of the $AlAs_{0.98}P_{0.02}$ layer was determined by X-ray diffraction using a Bruker D8 diffractometer.

After deposition, the wafers were cleaved in pieces of 10 × 10 mm. Then, a flexible carrier was mounted on top of the samples using double-sided tape. The samples were etched using a weight-induced ELO (WI-ELO) process (see Fig. 1a). Lift-off of the thin-film structure from its substrate was obtained by mounting the sample with its flexible carrier upside down on a support rod in a plastic container. A weight attached to the flexible carrier bends open the crevice between the substrate and the thin film with a radius of curvature of ~40 mm. The HF solution was stored in a separate reservoir of ~500 mL, the temperature of which could be regulated with an accuracy of ~0.5°C. From this reservoir, a continuous flow of HF solution at a temperature of 64.7°C was applied to one side of the sample. During etching, images of the sample were taken every ~1 s with a charge coupled device (CCD) camera to monitor the process and to measure the etch time required to completely release the thin film from the substrate (see also Ref. 12). After etching, the samples were rinsed in nanopure water and carefully blown dry with nitrogen.

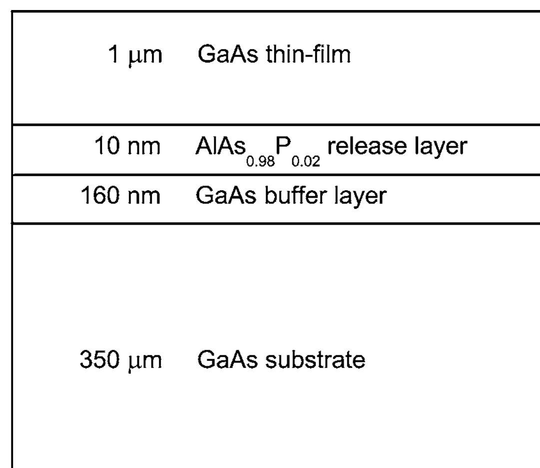

Figure 2. Schematic cross section of the layer structures with the thin-film GaAs layer and GaAs substrate (plus buffer layer) separated by an $AlAs_{0.98}P_{0.02}$ release layer.

To determine the ELO etch rate as a function of the O_2 concentration $[O_2]_{aq}$ in the HF solution an oxygen-nitrogen gas mixture with an adjustable $O_2/(O_2 + N_2)$ ratio was bubbled through the HF solution in the reservoir. The total gas flow of this mixture was kept constant at 2 L min^{-1} and was initiated one hour before each experiment. At equilibrium $[O_2]_{aq}$ can be described by[13]

$$[O_2]_{aq} = k_{O_2} P_{O_2} \quad [5]$$

with k_{O_2} the equilibrium constant and P_{O_2} the O_2 partial pressure. P_{O_2} can easily be determined using gas chromatography (GC). However, the HF saturated gas phase is detrimental to the GC equipment. Therefore, the HF solution in the reservoir was replaced by plain water to determine P_{O_2} as a function of the $O_2/(O_2 + N_2)$ ratio of the gas flowing through the solution. After stabilizing the flow for 1 h, 100 μL gas samples were taken from the plastic container of the ELO setup using a gas-tight syringe and injected into an Agilent 6890N GC. The gas compounds were divided over a HP Porapak Q Column (1.83 m long; 3.18 mm diam; 80/100 mesh) and a molecular sieve column (1.83 m long; 3.18 mm diam; 60/80 mesh) using helium as carrier gas at a flow of 24 and 8.4 mL min^{-1}, respectively. The separated compounds were quantified via a thermal conductivity detector. The temperatures of the injector, column, and detector were 125, 65, and 200°C, respectively. The results show that P_{O_2} increases linearly with the $O_2/(O_2 + N_2)$ ratio and that the lowest and highest O_2 partial pressures reached were 0.003 and 0.98 atm, respectively, the former indicating that the oxygen cannot be completely excluded from the solution and the reservoir.

In the present work, the concentrations of the species in the HF solution were calculated as a function of C_{HF} and T. Furthermore, in a first series of experiments, the ELO etch rate was studied for HF solutions with C_{HF} ranging from 0 to 24 mol kg^{-1} at P_{O_2} = 0.21 atm (air). In a second series of experiments, the ELO etch rate with a C_{HF} = 10 mol kg^{-1} (or 20% HF) solution was studied with P_{O_2} varying between 0 and 1 atm. For each process condition, five samples were examined and used to determine the average lateral etch rate and corresponding standard deviation.

Results and Discussion

Calculated composition of aqueous HF solutions.— HF is a weak acid and is not fully dissociated in an aqueous solution. Moreover, it can form with F^- and undissociated HF, the species HF_2^- and $H_2F_3^-$, respectively. At 25°C, the equilibrium constants for the system are[14,15]

Downloaded 16 Jan 2009 to 131.211.45.133. Redistribution subject to ECS license or copyright; see http://www.ecsdl.org/terms_use.jsp

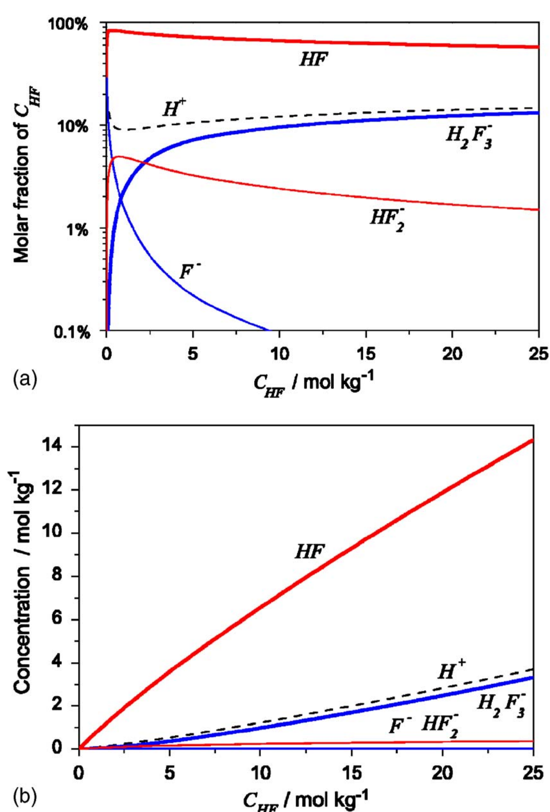

Figure 3. (Color online) (a) The calculated molar fraction of the species (H^+, F^-, HF, HF_2^-, $H_2F_3^-$) in an aqueous HF solution as a function of the total HF concentration at 65°C. (b) The calculated absolute concentration of the HF species as a function of C_{HF} at 65°C.

$$\frac{[H^+][F^-]}{[HF]} = 6.85 \times 10^{-4} \text{ mol kg}^{-1}$$

$$\frac{[HF_2^-]}{[HF][F^-]} = 5.0 \text{ kg mol}^{-1}$$

$$\frac{[H_2F_3^-]}{[HF][HF_2^-]} = 0.58 \text{ kg mol}^{-1} \quad [6]$$

These equilibrium constants (K_{eq}) depend on the temperature according to

$$K_{eq} = \exp\left(\frac{-\Delta\mu}{k_B T}\right) \quad [7]$$

where $\Delta\mu$ is the difference in Gibbs free energy. Furthermore, following the conservation of charge the proton concentration must be equal to the total concentration of the negative fluoride ions F^-, HF_2^-, and $H_2F_3^-$

$$[H^+] = [F^-] + [HF_2^-] + [H_2F_3^-] \quad [8]$$

and according to the conservation of mass the total concentration of species in the HF solution depends on C_{HF}, as described by

$$[F^-] + [HF] + 2[HF_2^-] + 3[H_2F_3^-] = C_{HF} \quad [9]$$

Equations 6-9 can be used to calculate the concentrations of the species in the HF solution as a function of C_{HF} and T. Since it is difficult to determine analytically the concentration of these species, the equations were solved numerically. In Fig. 3a, the molar fraction of the species with respect to C_{HF} is plotted as a function of C_{HF} at 65°C. The most abundant species for HF solutions with $C_{HF} > 1$ mol kg^{-1} is HF. In Fig. 3b, the absolute concentration of the species is plotted as a function of C_{HF} at 65°C. For HF solutions between 0 and 25 mol kg^{-1}, the concentration of the HF molecules increases almost linearly from 0 to 14 mol kg^{-1}. It should be noted, however, that the use of concentrations instead of activities leads to small inaccuracies due to the nonideal nature of fluoride solutions.[14]

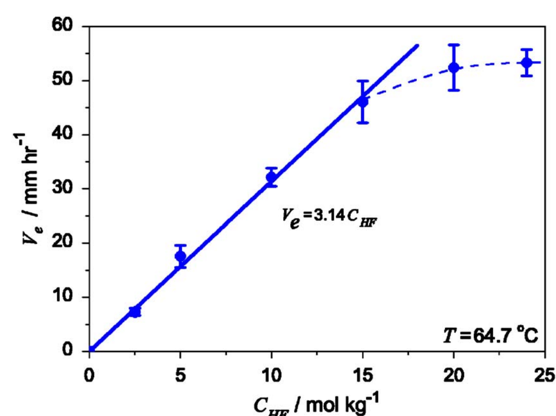

Figure 4. (Color online) Lateral etch rate of the ELO process as a function of the total HF concentration in solution. The width of the error bars is given by the standard deviation. The dashed line is to guide the eye and the solid line indicates the best linear fit through the data obtained for C_{HF} up to 15 mol kg^{-1}.

Influence of HF species.— The lateral etch rate of the ELO process is shown in Fig. 4 as a function of C_{HF}. Over a C_{HF} range varying from 0 to 15 mol kg^{-1}, the etch rate increases linearly from 0 to about 45 mm h^{-1}. This linear dependence is in accordance with the DR-model (see Eq. 2). The best linear fit through the data points up to C_{HF} = 15 mol kg^{-1} is given by

$$V_e = 3.14 C_{HF} \quad [10]$$

with V_e the etch rate in millimeter per hour.

In a previous work,[8] it was suggested that the first step in etching of AlAs by aqueous HF could be due to either the dissociated species (H^+ and F^- ions) or the undissociated acid (HF, HF_2^-, and $H_2F_3^-$) as shown in Fig. 5a and b, respectively. Because of the difference in electronegativity of Al and As, the Al–As surface bond is expected to be polarized. Proton attack on the "negatively charged" As leads to the rupture of the Al–As bond and the formation of a new As–H bond (step 1 of Fig. 5a). At the same time, the positively charged Al can be complexed by either F^- (step 2) or H_2O (step 3). If the remaining back bonds to As and Al react in the same way as in steps 1–3, then AsH_3 and either AlF_3 or $Al(H_2O)_n^{3+}$ will be formed. Alternating attack on a surface Al atom by F^- and H_2O will give rise to a mixed fluoro-aqua complex $[AlF_n(H_2O)_{(6-n)}]^{(3-n)+}$, with n = 1,2,3. In principle, attack on a surface Al–As bond by the undissociated acid, as occurs for InP in HCl,[16] is also possible (see Fig. 5b). This leads to the rupture of an As–Al bond, and the formation of an As–H and an Al–F bond in a single step. The result will be the same as for step 2 of Fig. 5a. Subsequent reactions with F^- or HF and/or H_2O will lead to the same products.

In order to explain the experimentally obtained ELO etch rates, it was concluded in a previous study[9] that the etch process is determined by an HF species with a concentration close to that of the total HF solution. If it is assumed that the equilibrium reactions between the dissociated and undissociated HF species are slow compared to the AlAs reaction with these species, then the contribution of each mechanism to the actual etch process can be determined by comparing the concentration of dissociated HF species with that of the undissociated HF species. Figure 3 shows that for C_{HF} above 1 mol kg^{-1}

Downloaded 16 Jan 2009 to 131.211.45.133. Redistribution subject to ECS license or copyright; see http://www.ecsdl.org/terms_use.jsp

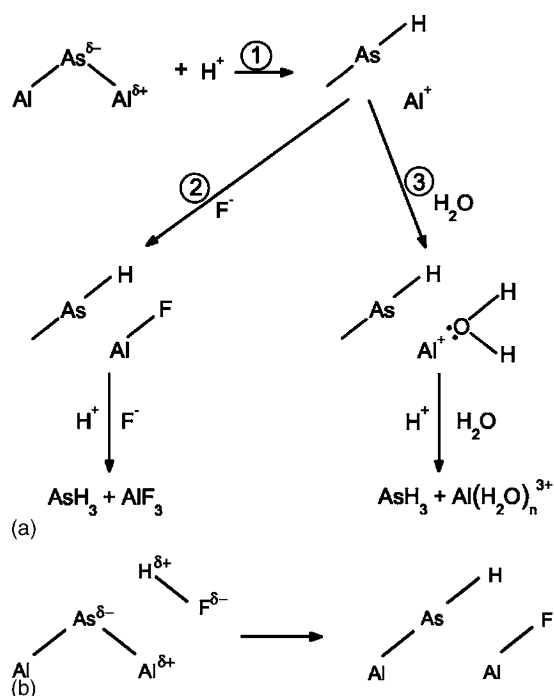

Figure 5. Schematic representation of the reaction mechanisms for the etching of AlAs (a) with dissociated HF and (b) with undissociated HF.

$$[H^+] + [F^-] \ll [HF] + [HF_2^-] + [H_2F_3^-] \quad [11]$$

indicating that the first step in etching of AlAs by aqueous HF must occur predominantly by the attack of the undissociated acid. This leads to the rupture of an As–Al bond, and the formation of an As–H and an Al–F bond in a single step. In view of the high concentrations of undissociated HF species, the majority of the further reaction mechanism is also expected to be similar to the etching of InP in a concentrated HCl solution.[16] This means that subsequent reactions with undissociated acid lead to the formation of AsH_3 and AlF_3

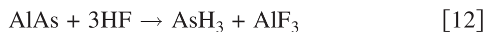

$$AlAs + 3HF \rightarrow AsH_3 + AlF_3 \quad [12]$$

in which AlF_3 is subsequently hydrolyzed.

As shown in Fig. 4, for $C_{HF} = 20$ and 24 mol kg^{-1} etch rates were found of 52 ± 4 and 53 ± 2 mm h^{-1}, respectively. These data points show a clear deviation from the linear fit, which indicates that the ELO process is limited in some way not accounted for by the DR-model. This could be the relatively slow or incomplete dissolution of reaction products under these particular conditions resulting in an accumulation of reaction products close to the etch front.[9] According to Eq. 1, the ELO process overall requires 3 moles of HF and 3–6 moles of H_2O per mole of AlAs. This implies that for the chemical attack of the release layer and subsequent dissolving of reaction products to transport them away from the etch front both HF and H_2O molecules are required in a ratio of about 1:2 (see Eq. 1). Of course, there is more than sufficient HF and H_2O in the total solution but because the exchange of molecules through the narrow slit leading to the etch front (see Fig. 1) is difficult, the local ratio of molecules at the etch front becomes an important factor in the etch process. In Fig. 6, the total water concentration C_{H_2O} is plotted as a function of C_{HF}. According to Fig. 6, there is an excess of H_2O compared to the total HF for solutions with a relatively low C_{HF} and the dissolution of the reaction products is not expected to slow down the overall ELO process rate. For increasing C_{HF} values, however, the C_{H_2O}/C_{HF} ratio reduces and, consequently, the dissolution and removal rate of the reaction products is expected to reduce. The subsequent accumulation of reaction products at the etch front adds to the total resistance of the ELO process (see Eq. 2-4) that is not accounted for in the DR-model. This mechanism provides a possible explanation for the fact that for $C_{HF} > 15$ mol kg^{-1}, the ELO etch rates show a clear deviation from its linear relation with C_{HF}. However, further research is required to determine the exact role of water on the etch mechanism. It should be noted that in an aqueous solution, there is much controversy over the nature of undissociated HF and questions about whether it actually exists as a complex with a water molecule. Therefore, it would be interesting to replace the water solvent with acetonitrile for a following study.

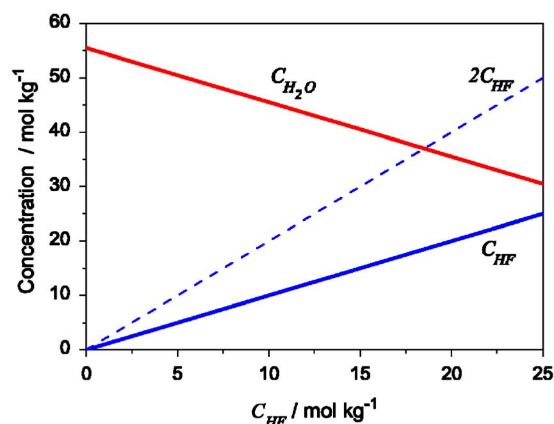

Figure 6. (Color online) The total water concentration and the total HF concentration in an aqueous HF solution as a function of C_{HF} at 25°C.

Influence of oxygen.— Previous work[8] showed that oxygen (O_2) is required to maintain the AlAs etch process with HF. Therefore, the influence of oxygen on the ELO etch process was investigated by bubbling an oxygen/nitrogen gas mixture with a variable $O_2/(O_2 + N_2)$ ratio through the etch solution. In Fig. 7, the lateral etch rate is shown as a function of P_{O_2} in the HF reservoir. Over a P_{O_2} range varying from 0.046 to 0.98 atm, the etch rate increases slightly from 32 ± 3 to 40 ± 2 mm h^{-1} with the O_2 partial pressure. The best linear fit through these data points yields

$$V_e = 10.1P_{O_2} + 31.6 \quad [13]$$

For $P_{O_2} = 0.003$ atm, however, a markedly lower ELO etch rate of 12 ± 1 mm h^{-1} was found. These results are in line with previous work,[8] where bulk etch experiments performed in an O_2-rich atmosphere showed an AlAs etch rate ~30% higher than in an O_2-poor

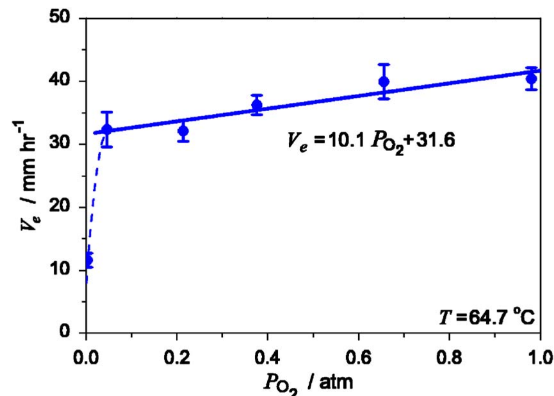

Figure 7. (Color online) Lateral etch rate of the ELO process as a function of the O_2 partial pressure in the reservoir of the HF solution. The width of the error bars is given by the standard deviation. The dashed line is a guide to the eye, and the solid line indicates the best linear fit through the data obtained over a P_{O_2} range varying from 0.046 to 0.98 atm.

Downloaded 16 Jan 2009 to 131.211.45.133. Redistribution subject to ECS license or copyright; see http://www.ecsdl.org/terms_use.jsp

atmosphere, and a premature halt of etching ($V_e = 0$) in a 100% N_2 atmosphere. This indicates that O_2 maintains the ELO process in some way.

To discuss the role of O_2 in the ELO process, information is required on the solubility and diffusion data of O_2 in HF solutions. Unfortunately, we were unable to trace these data in the literature, so we now use instead data related to the solubility and diffusion of O_2 in water from Ref. 13 and 17 ($k_{O_2} = 8.51 \times 10^{-4}$ M atm^{-1} at 338 K for $P_{O_2} = 1$ atm, $D = 2.42 \times 10^{-5}$ cm^2 s^{-1} at 298 K and $E_{a,d}$ is calculated to be 0.27 eV) to approximate the diffusion of O_2 in a 20% HF solution. Using Eq. 5, the solubility of dissolved O_2 is calculated to be 1.79×10^{-4} M in an ambient atmosphere ($P_{O_2} = 0.21$ atm). Note, that $[O_2]_{aq}$ is ~ 5 orders of magnitude lower than the total HF concentration of 10.5 M (10 mol kg^{-1}) for a 20% HF solution. Hence, in a similar way as derived in previous work,[9] it is found that O_2 diffusion would limit the ELO etch rate to a maximum of only a few micrometers per hour if it was required in the dominant reaction with AlAs. Because the experimentally obtained etch rates are several orders of magnitude larger, it is clear that O_2 cannot be directly involved in this process.

In previous work,[8] an AlAs bulk etch experiment was performed with a $C_{HF} = 0.25$ mol kg^{-1} HF solution in a 100% N_2 atmosphere. The process suddenly stopped after etching 60–70% of the total amount of AlAs. It was suggested that the AlAs surface might be blocked or passivated by the formation of elemental As. Therefore, we assume that the passivation observed in an oxygen-poor atmosphere is caused by the formation of some elemental As at the etch front. This process is most likely the reaction of AlAs with protons (H^+) leading to the formation of hydrogen (H_2) and oxidized Al

$$2AlAs + 6H^+ \rightarrow 2As + 2Al^{3+} + 3H_2 \qquad [14]$$

The Al^{3+} ions may subsequently react with the solution, as described in the previous section, leaving the elemental As at the surface. The stable form of As is As_4, but two arsenic atoms may also form the metastable As_2 molecule. One would therefore expect the formation of either As_2 or As_4 at the surface layer passivating the etching process in the absence of dissolved O_2 in the HF solution. The experiments clearly demonstrate the influence of the presence of oxygen during the etching process: preventing passivation and maintaining the etch process. According to the electrochemical series of Ref. 17, an oxidation reaction leading to the formation of arsenic trioxide (As_2O_3) can be described by

$$4As + 3\ O_2 \rightarrow 2As_2O_3 \qquad [15]$$

Using Eq. 14 and 15, the overall reaction to describe the passivation/oxidation process is given by

$$4AlAs + 12H^+ + 3\ O_2 \rightarrow 2As_2O_3 + 4Al^{3+} + 6H_2 \qquad [16]$$

in which Al^{3+} subsequently reacts with H_2O and/or HF to yield one of the aluminum fluoride complexes (see Eq. 1). In previous work[8] on the AlAs bulk etching with HF solutions, besides AsH_3 and the aluminum fluoride complexes as the major reaction products, small amounts of hydrogen (H_2) and oxidized arsenic (probably As_2O_3) were also found.

These results correlate well with the description of the ELO etch process given in the present work, i.e., a primary etch process according to Eq. 1, supported by a secondary reaction according to Eq. 16. Based on the concentration of H^+ compared to that of the undissociated HF (see Fig. 3), one would estimate that maximally $\sim 10\%$ of the AlAs etching proceeds according to the secondary process yielding elemental arsenic as an intermediate product. This indicates that the AlAs reaction with (undissociated) HF is scarcely obstructed by the passivation/oxidation reaction under the usually applied conditions which indicates that HF can etch around the elemental arsenic. However, under oxygen-poor conditions a passivating arsenic film can develop, which covers the etch front and completely blocks the AlAs reaction with HF after a certain period of time.

Conclusion

The lateral etch rate of the AlAs release layer in the ELO process was determined as a function of C_{HF} in the aqueous HF solution. Over a C_{HF} range varying from 0 to 15 mol kg^{-1}, it was found that the etch rate increases linearly with the total HF concentration. This dependence is in accordance with the DR-model as presented in previous work. However, for $C_{HF} > 15$ mol kg^{-1}, the etch rate levels off. This is probably related to a limited dissolution of the aluminum fluoride products under these conditions.

The results of these experiments and the distribution of species in the aqueous HF solution, as numerically calculated, show that the first step in the etch process of AlAs with an HF solution most probably takes place by chemical attack of undissociated HF on AlAs surface bonds. After subsequent reactions with HF, this gives rise to the formation of AsH_3 and (hydrated) AlF_3. In principle, the mechanism is similar to the etching of InP in a concentrated HCl solution, in which PH_3 and $InCl_3$ are formed.

In a second series of experiments the ELO process was studied as a function of P_{O_2}. Over a P_{O_2} range varying from 0.046 to 0.98 atm, the etch rate increases slightly with the O_2 partial pressure. For $P_{O_2} = 0.003$ atm, however, a significantly lower ELO etch rate is found. According to the present work, the observed decrease is the result of surface passivation by elemental arsenic, which is formed by the reaction of AlAs with H^+. An oxygen-poor atmosphere may allow the buildup of elemental arsenic on the surface and thus slow down the AlAs reaction with HF; oxygen removes arsenic as As_2O_3. The distribution of species in the aqueous HF solution as numerically calculated shows that the probability for surface passivation by elemental arsenic is low. This indicates that the DR-model, which was derived in a previous study, gives a realistic description of the ELO process under the generally applied WI-ELO conditions.

Acknowledgments

The authors thank W. H. M. Corbeek for his technical support regarding the construction of the WI-ELO setup. This work was financially supported by the Dutch Technology Foundation STW under project no. NET.7452.

Radboud University Nijmegen assisted in meeting the publication costs of this article.

References

1. G. J. Bauhuis, J. J. Schermer, P. Mulder, M. M. A. J. Voncken, and P. K. Larsen, *Sol. Energy Mater. Sol. Cells*, **83**, 81 (2004).
2. A. van Geelen, P. R. Hageman, G. J. Bauhuis, P. C. van Rijsingen, P. Schmidt, and L. J. Giling, *Mater. Sci. Eng., B*, **45**, 162 (1997).
3. Y. Yazawa, J. Minemura, K. Tamura, S. Watahiki, T. Kitatam, and T. Warabisako, *Sol. Energy Mater. Sol. Cells*, **50**, 163 (1998).
4. J. Maeda, Y. Sasaki, N. Dietz, K. Shibahara, S. Yokoyama, S. Miyazaki, and M. Hirose, *Jpn. J. Appl. Phys., Part 1*, **36**, 1554 (1997).
5. Y. Sasaki, T. Katayama, T. Koishi, K. Shibahara, S. Yokoyama, S. Miyazaki, and M. Hirose, *J. Electrochem. Soc.*, **146**, 710 (1999).
6. G. J. Bauhuis, P. Mulder, J. J. Schermer, E. J. Haverkamp, J. van Deelen, and P. K. Larsen, in *Proceedings of the 20th European Photovoltaic Solar Energy Conference*, Barcelona, p. 468 (2005), http://www.photovoltaic-conference.com
7. M. A. Green, K. Emery, D. L. King, S. Igari, and W. Warta, *Prog. Photovoltaics*, **13**, 387 (2005).
8. M. M. A. J. Voncken, J. J. Schermer, A. T. J. van Niftrik, G. J. Bauhuis, P. Mulder, P. K. Larsen, T. P. J. Peters, B. de Bruin, A. Klaassen, and J. J. Kelly, *J. Electrochem. Soc.*, **151**, G347 (2004).
9. A. T. J. van Niftrik, J. J. Schermer, G. J. Bauhuis, P. Mulder, P. K. Larsen, and J. J. Kelly, *J. Electrochem. Soc.*, **154**, D629 (2007).
10. E. Yablonovitch, T. Gmitter, J. P. Harbison, and R. Bhat, *Appl. Phys. Lett.*, **51**, 2222 (1987).
11. M. M. A. J. Voncken, J. J. Schermer, G. Maduro, G. J. Bauhuis, P. Mulder, and P. K. Larsen, *Mater. Sci. Eng., B*, **95**, 242 (2002).
12. A. T. J. van Niftrik, J. J. Schermer, G. J. Bauhuis, J. van Deelen, P. Mulder, and P. K. Larsen, *Cryst. Growth Des.*, Accepted.
13. D. Tromans, *Hydrometallurgy*, **48**, 327 (1998).
14. K. W. Kolasinski, *J. Electrochem. Soc.*, **152**, J99 (2005).
15. K. W. Kolasinski, *J. Electrochem. Soc.*, **153**, L28 (2006).
16. P. H. L. Notten, *J. Electrochem. Soc.*, **131**, 2641 (1984).
17. *CRC Handbook of Chemistry and Physics, Internet Version 2007*, 87th edition, D. R. Lide, Editor, http://www.hbcpnetbase.com.

Downloaded 16 Jan 2009 to 131.211.45.133. Redistribution subject to ECS license or copyright; see http://www.ecsdl.org/terms_use.jsp